JJMIE

Volume 4, Number 1, Jan. 2010
ISSN 1995-6665
Pages 155- 162

Jordan Journal of Mechanical and Industrial Engineering

Numerical Modeling of Coal Tire-Shred Co-Gasification

Ilham Talab, Zaki Al-Nahari, Rana Qudaih, Isam Janajreh *

Mechanical Engineering Program, Masdar Institute of Science & Technology (MIST), Sas Al Nakhl Area

Abu Dhabi, Abu Dhabi, P.O.Box 54224,United Arab Emirates

Abstract

Tires, plastics, cellulosic materials, i.e., papers and cardboards are rich in hydrocarbon yet land filling of the waste of these materials is still practiced causing potential risk to our ecosystem through gas emissions (essentially CH_4) and ground water leaching. Co-Gasification within the existing infrastructure of pulverized coal utility gasifiers is considered a practical near-term solution for these rich hydrocarbon waste materials while minimizing capital requirements and maintaining the high efficiency of pulverized coal reactors. Systematic and numerical modeling of coal/tire shred fuel blend gasification is presented in this study. Co-combustion and gasification of tire shred and coal is a complex problem that involves gas and particle phases, along with the effect of turbulence on the chemical reactions. Coal/tire shred gasification modeling involves the prediction of volatile evolution and char burnout from the co-pulverized coal/biomass particles along with simulation of the gasification chemistry occurring in the gas phase. The mathematical models used for co-pulverized coal/tire shred particle gasification consist of models for turbulent flow (RNG k-ε model); gas phase gasification (Species Transport model); particles dispersion by turbulent flow (Cloud Tracking model); coal/biomass particles devolatilization (Constant Rate model); heterogeneous char reaction (Multiple surface reactions model); and radiation (Discrete Ordinates model). The coal was blended with 5, 10, and 20% tire shred (mass basis) for co-gasification. The effect of the percentage of tire shred blended with coal on the temperature distribution, products distribution, particle burnout rate, and pollutant emissions at the exit of the furnace will be presented.

Keywords: Cogasification, numerical modeling, systematic modeling, char-burnout.

1. Introduction

A relatively new technology for electricity production that is gaining prominence in the world is that of gasification. Waste tires and coal co-gasification within the existing infrastructure of pulverized coal utility boilers or gasifiers is viewed as a practical near-term means of encouraging renewable energy while minimizing capital requirements and maintaining the high efficiency of pulverized coal boilers/gasifiers [1-3]. The wide availability of pulverized coal boilers (in number and capacity) translates into significant opportunities for waste tire utilization even at levels of only 5 to 20% of thermal input. Coal/tire co-gasification has several benefits: it is the fastest way to increase the use of the humongous quantities of tire disposed every year for electric power generation; it saves capital cost by utilizing existing plant infrastructure; and it offers environmental advantages, such as reducing No_x emissions [4]. Co-pulverized coal and tire particles gasification modeling is a complex problem that involves gas and particle phases along with the effect of turbulence on the chemical reactions. In addition to solving the transport equations for the continuous phase (gas), the discrete second phase (spherical solid particles) in the Lagrangian frame of reference is also predicted. Discrete phase modeling is used for the prediction of particle trajectories and the individual conservation equations for the chemical species are solved utilizing the species convection-diffusion equation.

Corresponding Authors. ijanajreh@masdar.ac.ae.

  - Volume 4, Number 1 (ISSN 1995-6665)

2. Governing Equations and Solution Procedures

Modeling of gasification involves the application of conservation laws, and accounting for volatile evolution, char particles burnout, and coupling the homogeneous chemistry occurring in the gas phase as well as the heterogeneous in the solid phase.

Systematic Analysis Equations:
Systematic analysis or zero-dimension-modeling is an equilibrium analysis which quantitatively estimates the associated oxidizer and moderator feedstreams and syngas yields in the case of gasification. It predicts species and determines the needed oxygen and moderator (CO_2 or H_2O) per mole of feedstock at the operating temperature and pressure of a given gaisifier. There are several gasification technologies that classified according to their operating temperature as low, intermediate, and high temperature such as fixed bed (moving bed) gasifier, fluidized bed gasifier and entrained flow gasifier, respectively. The high operating temperature (~1250-1600°C) of the entrained flow gasifier reduces the residence time that make them popular for high throughput application. Entrain gasifiers are amenable for equilibrium due to the fast chemical reactions and the calculations of syngas composition are reasonably accurate [5]. Whether accommodating pulverized solid hydrocarbon or in slurry and with the addition of oxidizer, the goal of systematic analysis is to determine the equilibrium species concentrations as well as the temperature and pressure of the products. While the reactions consist of several hundreds of steps and hundreds of species and radicals, the following general three step reactions represent the predominant reaction pathway.

$$\begin{aligned}
&\text{water gas reaction} && C_{(solid)} + H_2O \underset{k_{b,r}}{\overset{k_{f,r}}{\Leftrightarrow}} CO + H_2 && +131\,MJ/Kmole & \quad (1a)\\
&\text{Boudouard reaction} && C_{(solid)} + CO_2 \underset{k_{b,r}}{\overset{k_{f,r}}{\Leftrightarrow}} 2CO && +173\,MJ/Kmole & \quad (1b)\\
&\text{Methanation reaction} && C_{(solid)} + 2H_2 \underset{k_{b,r}}{\overset{k_{f,r}}{\Leftrightarrow}} CH_4 && -75\,MJ/Kmole & \quad (1c)
\end{aligned} \quad (1)$$

The feedstock (whether is mixed or homogenous) consumes all the available oxygen in a series of three heterogeneous reactions. In the above reactions the feedstock is represented by a solid carbon and the products are limited to six species (unconverted solid $C_{(solid)}$, CO,CO_2, CH_4, H_2, and H_2O). The Methanation reaction is several orders of magnitude slower than the Boudouard and Water gas reactions (Smooth and Smith 1985). Each of these reaction equations is independent, and has an associated equilibrium equation in terms of either their molar concentration or partial pressure as follow:

$$K_c(T) = \frac{[C]^c[D]^d}{[A]^a[B]^b} \quad or\ K_p(T) = \frac{p_C^c . p_D^d}{p_A^a . p_B^b} \quad (2)$$
$$and K_c(T) = K_p(T).(RT)^{c+d-a-b}$$

Where [X] indicates the molar concentration of species X, lower case c, d, a , and b are the stoichiometric coefficients, and K_c is generally expressed in Arrhenius rate as:

$$k_c(T) = A_r T^{\beta_r} e^{-\frac{E_r}{RT}} \quad (3)$$

where A_r is the pre-exponent constant, β is temperature exponent constant, E_r is the activation energy, R is the universal gas constant (R = 8.313kJ/kmol. K), T is the absolute temperature. At equilibrium K_c is expressed in terms of Gibbs free energy ($\Delta g^o = \Delta h^o - T\Delta s^o$) that ties 1st and 2nd thermodynamic quantities to indicate reaction spontaneousity as:

$$k_c(T) = e^{-\frac{\Delta g^o}{RT}} \quad (4)$$

Where Δh_o and Δs_o are the standard enthalpy and entropy change of reactions. The three elemental mass conservation equations for C, H and O add another three equations to the three reactions equilibrium equations. The total molar fractions and energy equation warrant the solution of the system (6 species and any two variables of four: Temperature, pressure, and moderator oxidizer molar concentration per mole of feedstock). The steady form of the energy equation is written as:

$$\sum_{i=1}^{n\ product} \dot{n}_i h_i = \sum_{i=1}^{n\ reactant} \dot{n}_i h_i + \dot{Q} \quad (5)$$

Where the enthalpy terms, h, include enthalpies of formation and sensible enthalpies.

Continuous Phase and CFD Equations:
The continuous phase is governed by Navier-Stoke equation that associated with source term:

$$\underset{Time\ rate}{\frac{\partial}{\partial t}(\phi)} + \underset{advective}{\frac{\partial}{\partial x_i}(u_i\phi)} = \underset{diffusion}{-\frac{\partial}{\partial x_i}\left(\Gamma_\phi \frac{\partial \phi}{\partial x_i}\right)} + \underset{source}{S_\phi} \quad (6)$$

where ρ is the density and upper case S_φ is the source terms due to the dispersed/discrete phase interaction. Φ is the dependent variable corresponding to density (ρ), the density velocity multiple (ρ,ui), and the temperature (T), representing the conservation of mass, momentum, and energy respectively. Φ can also represent turbulent scalars, i.e. turbulent kinetic energy (k) and turbulent dissipation rate (ε). These two equations in steady state flow regime are written as:

$$\begin{aligned}
&\rho u_i \frac{\partial k}{\partial x_i} = \mu_t \left(\frac{\partial u_j}{\partial x_i} + \frac{\partial u_i}{\partial x_j}\right)\frac{\partial u_j}{\partial x_i} + \frac{\partial}{\partial x_i}\left(\frac{\mu_t}{\sigma_k}\frac{\partial k}{\partial x_i}\right) - \rho\varepsilon\\
&\rho u_i \frac{\partial \varepsilon}{\partial x_i} = C_{1z}\frac{\mu_t \varepsilon}{k}\left(\frac{\partial u_j}{\partial x_i} + \frac{\partial u_i}{\partial x_j}\right)\frac{\partial u_j}{\partial x_i} +\\
&\frac{\partial}{\partial x_i}\left(\frac{\mu_t}{\sigma_z}\frac{\partial \varepsilon}{\partial x_i}\right) - C_{2z}\frac{\rho\varepsilon^2}{k}
\end{aligned} \quad (7)$$

The right hand terms represent the generation, the diffusion, and destruction respectively. In these equations, μ_t is the turbulent or eddy viscosity $\mu_t = f_\mu C_\mu \rho k^2/\varepsilon$. Where f and C are constants and C_{1z}, C_{2z}, σ_κ, and σ_z, are empirical constants. The transportation of species m_i is written as:

$$\frac{\partial}{\partial t}(\rho m_i) + \frac{\partial}{\partial x_i}(\rho u_i m_i) = \frac{\partial}{\partial x_i}\left(\rho D_{i,m} + \mu_t / Sc_t\right)\frac{\partial m_i}{\partial x_i} + R_i + S_i \quad (8)$$

Where $D_{i,m}$ is the diffusion coefficient. Sc_t is the turbulent Schmidt number which is a ratio of the eddy viscosity μ_t to the eddy diffusivity $D_{ti,m}$. These transport equations

incorporate a reaction source term R_i in addition to the S_i which accounts for discrete phase interaction. The R_i term is governed by the stoichiometric reaction below:

$$\sum_{i=1}^{N} v'_{i,r} S_i \underset{k_{b,r}}{\overset{k_{f,r}}{\Leftrightarrow}} \sum_{i=1}^{N} v''_{i,r} S_i \quad (9)$$

The i^{th} species production/destruction due to the reaction r is written as:

$$R_{i,r} = M_{i,r}(v''_{i,r} - v'_{i,r})\left(k_f \prod_{j=1}^{N} [C]_{j,r}^{\eta^*_{rj}} - k_b \prod_{j=1}^{N} [C]_{j,r}^{v''_{j,r}} \right) \quad (10)$$

where k is the reaction constant described in equation 3, and $[C]_j$ is the molar concentration of j_{th} specie raised to stoichiometric coefficients ν and reaction order η, and M_i is the molecular weight of species i.

Discrete Modeling Justification:

Gasification processes are typically turbulent and hence require modeling avoiding the exhaustive and numerical intensive direct numerical simulation (DNS). For example the length scale, velocity and Reynolds number of gas turbine combustor, after burner, and utility furnace are (0.1m, 50m/s, 250,000), (0.5m, 100m/s, 2,500,000), and (10m, 10m/s, 5,000,000) respectively. The smallest turbulent scale, known as Kolmogorov scale, denoted with η is expressed as:

$$\eta = L \,.\, \mathrm{Re}^{-\frac{3}{4}} \quad (11)$$

where L is the characteristic length scale. Solving the flow field down to η scale requires $\mathrm{Re}^{9/4}$ computational node for each dimension, $\mathrm{Re}^{9/4}$ nodes for three dimensional, and it is impractical at Re=10,000 (10^9 nodes). The discrete Lagrangian method is used for the solid phase. At low volume fraction (α) the average particle distance is greater than twice its diameter, therefore, particle-particle interaction can be neglected. Small particulate loading $(\alpha_d \rho_d / \alpha_c \rho_c << 1)$ implies a reasonable one-way coupling. Small value of the Stokes number (Ratio of the dispersed phase relaxation time $\tau_d = \alpha_d d_d^2 / 18\mu_c$ to that of the flow time $(\tau_c = U/D)$ indicates particles will closely follow the fluid, otherwise particles will move independently of the flow field.

Discrete/Particulate Phase Equations:

The discrete phase is solved in a Lagrangian frame of reference. This phase consists of spherical particles of 10μm to 100μm in diameter dispersed in the continuous phase. Their trajectory is predicted by integrating the force balance on the particle. This force balance equates the particle inertia with the forces acting on the particle and can be described as:

$$\frac{d\vec{u}_P}{dt} = F_D(\vec{u} - \vec{u}_P) + \vec{g}(\rho_P - \rho)/\rho_P + \vec{F} \quad (12)$$

Where F_D $(u - u_p)$ is the drag force per unit particle mass; u is the fluid phase velocity; u_p is the particle velocity; ρ is the fluid density, and ρ_p is the density of the particle. Equation (12) incorporates additional forces (F) in the particle force balance that can be important (thermophoretic and Brownian forces). The trajectory equations are solved by stepwise integration over discrete time steps. Integration of Eq. (12) yields the velocity of the particle at each point along the trajectory, with the trajectory itself predicted by

$$\frac{dx}{dt} = u_P \quad (13)$$

Equations similar to (12) and (13) are solved for each coordinate direction to predict the trajectories of the discrete phase. The trajectories of the discrete phase particles are computed as well as the heat and mass transfer to and from them. Inert heating law is applied while the particle temperature is less than the vaporization temperature. Devolatilization law is applied to the combusting particle mass (m_p) when the temperature of the particle reaches the vaporization temperature, T_{vap} . It is written as:

$$-\frac{dm_p}{dt} = Ae^{-(E/RT)}[m_p - (1 - f_v^0)m_p^0] \quad (14)$$

Where $f_{v,}$ and $m_p{}^o$ are the volatile fraction and initial mass, respectively. It remains in effect while the mass of the particle, m_p, exceeds the mass of the non-volatiles in the particle.

The heat transfer to the particle during devolatilization process governs the contributions from convection, radiation, and the heat consumed during devolatilization. It is written as:

$$m_p c_p \frac{dT_p}{dt} = hA_p(T_\infty - T_p) + \frac{dm_p}{dt} h_{fg} + \varepsilon_p A_p \sigma(T_R^4 - T_p^4) \quad (15)$$

Where c_p, $h_{fg,}$ ε, A, and σ are after the volatile component of the particle is completely evolved, a surface reaction begins, which consumes the combustible fraction of the particle until the combustible fraction is consumed. Heat, momentum, and mass transfer between the solid fuel particles and the gas will be included by alternately computing the discrete phase trajectories and the continuous phase equations.

The reactive two phase flow modeling is achieved within the framework of Fluent code [13].

3. Results and Discussion

Systematic analyses results:

Table 1 shows the proximate and ultimate analysis of the fuels used in this study. The lower heating values for the 0%, 5%, 10% and 20% coal and tire fuel blends are 31.91, 32.03, 32.15, and 32.38 MJ/kg respectively. It is noted in the proximate analysis that the amount of volatile matter and the ash content increase while fixed carbon and moisture content decrease when the amount of tire fuel blended with coal increases. As for the ultimate analysis, the percentage by weight of carbon, oxygen, and nitrogen decrease and the percentage of hydrogen and sulfur to a lesser extend increase when the amount of tire fuel blended with coal increases.

Table 1 – proximate and ultimate analysis of the fuel.

	Coal	Tire	Coal + 5%Tire	Coal + 10% Tire	Coal + 20% Tire
Proximate Analysis					
Fixed Carbone	0.5292	0.2293	0.5142	0.4992	0.4692
Volatile	0.3666	0.6731	0.3819	0.3973	0.4279
Moisture	0.0200	0.0102	0.0195	0.0190	0.0180
Ash	0.0842	0.0874	0.0844	0.0845	0.0848
Total	1.0000	1.0000	1.0000	1.0000	1.0000
Ultimate Elemental Analysis					
Carbon	0.7315	0.7299	0.7314	0.7313	0.7312
Oxygen	0.1058	0.0977	0.1054	0.1050	0.1042
Hydrogen	0.0531	0.0690	0.0539	0.0547	0.0563
Nitrogen	0.0153	0.0026	0.0147	0.0140	0.0128
Sulfur	0.0101	0.0124	0.0102	0.0103	0.0106
Ash	0.0842	0.0883	0.0844	0.0846	0.0850
Total	1.0000	1.0000	1.0000	1.0000	1.0000

The three coal/tire blends are modeled at a baseline temperature and pressure of 1,250C^{o} and 30bars, respectively. Four co-firing conditions (0, 5%, 10%, and 20% tire/coal) sweeping three operating temperatures (1,250 $\pm$ 250C^{o}) were carried out. The results suggest that there is negligible or no effect of adding tire on the production of CO. Figure 1(a) for example shows similar trends for the three coal/tire fuel blends for CO production at various temperatures. However, as the tire percent blended with coal increases, more H_2 is produced as shown in figure 1(b) mainly due to the increase in hydrogen as tire content increase. On the other hand, systematic analysis results demonstrate trends in NH_3, and H_2S produced from each fuel blend as depicted in figure 2 (a & b).

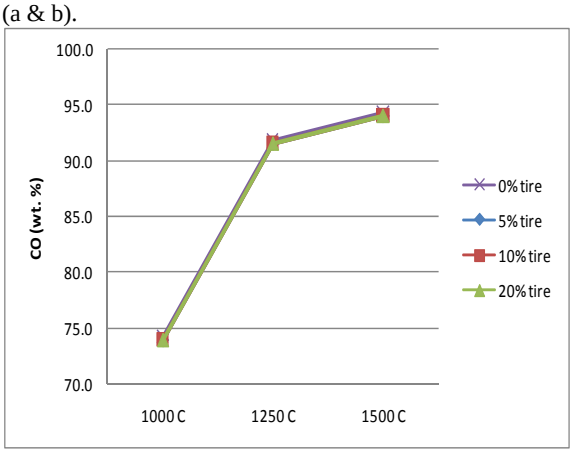

Fig. 1 (a). CO mass fraction.

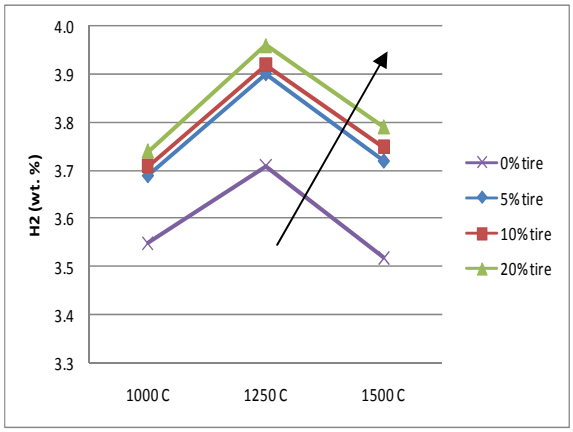

Fig. 1 (b). H_2 mass fraction.

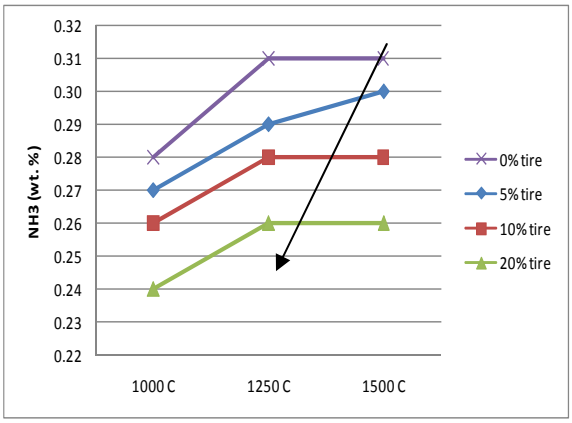

Fig. 2 (a). NH_3 mass fraction.

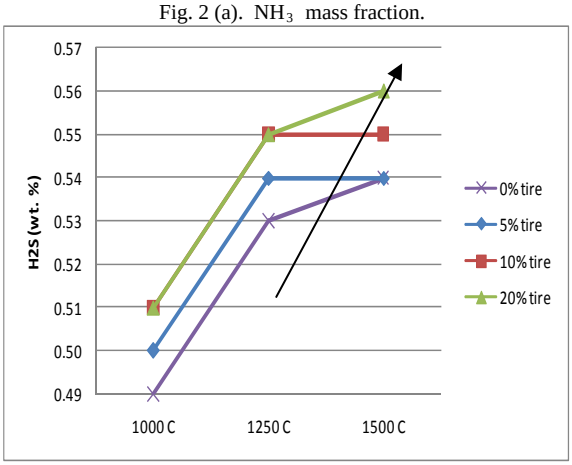

Fig. 2 (b). H_2S mass fraction.

Since the nitrogen content decreases as tire content increases in the fuel blend, it is anticipated that the formation of NH_3 will decrease as amount of tire blended with coal increases which is depicted in figure 2(a). Unlike nitrogen, sulfur content increases slightly as tire content increases and hence more H_2S is produced as percent of tire blended increases as shown in figure 2(b).

Reactive flow simulation results:

The geometry of the gasifier is depicted in figure 3. It was selected from the work of Chen et al. and Bockelie et al. [6,7,8,9]. The topology of the selected gasifier geometry is fitted with a multi-blocking mesh methodology. Multi-blocking provides a better grid resolution/clustering control, improves mesh structuring, and eases the use of the hexagonal mesh type for better inter cell communications and accuracy. The axisymmetrical meshing posses no complexity in construction, the 3-dimensional mesh, however, is more complex and must follow a general method that permits parametric studies without the need for reconstruction [10]. Flexibility in number of inlet ports, their radial distributions, and axial positioning are amongst the parameters that the 3 dimensional mesh is designed to offer.

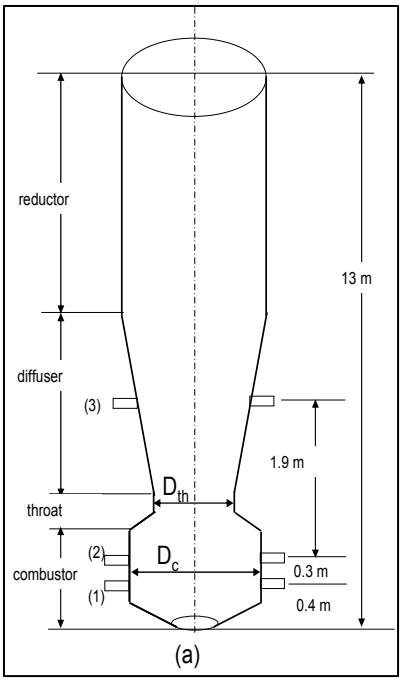

Fig. 3. Two-stage air blown gasifier and nozzle geometry.

The same fuel blends of coal with 5%, 10%, and 20% (mass basis) tire chips were studied assuming uniform particle diameter of 10 µm. For each case, the initial and boundary conditions were kept constant, and only the fuel composition had been changed. Table summarizes the boundary and operating conditions.

Table 2 – boundary and operating conditions.

Coal Feed	
Fuel flow rate (kg/s)	4
Fuel inlet temperature (K)	300
Oxidant & moderator: 23wt% O_2, 77wt% H_2O	
Flow rate at inlet 1 (m/s)	6
Flow rate at inlet 2 (m/s)	6
Flow rate at inlet 3 (m/s)	4
Turbulent intensity (%)	10
Flow inlet temperature (K)	1000
Gasifier pressure (bar)	30
Gasifier Wall temperature (K)	1600
Radiation model	Discrete Ordinates

The general conversion pathways of gasification can be summarized into the general global gas phase and solid phase reactions listed below [11, 12]:

$$Fuel \rightarrow CH_xO_yN_z + C_{(s)}Ash \quad (16)$$

For oxygen-rich conditions, combustion occurs:

$$CH_xO_yN_z + wO_2 \rightarrow CO_2 + \frac{x}{2}H_2O + zNO_2 \quad (17)$$

Where *w* can be readily calculated following simple elemental mass balance.

Heterogeneous reactions are:

$$C_{(s)}Ash + CO_2 \rightarrow 2CO + Ash \quad (18)$$

$$C_{(s)}Ash + H_2O \rightarrow CO + H_2 + Ash \quad (19)$$

$$C_{(s)}Ash + 2H_2 \rightarrow CH_4 + Ash \quad (20)$$

The volatiles react immediately to form CO_2 and H_2O in O_2 rich conditions at the bottom of the gasifier. The simulations revealed 100% conversion of both volatiles and char reactions. The effects of tire blended with coal on gas temperature; CO, NO emissions; and particle burnout rate, are discussed next.

The results show a higher gas temperature for lower tire content fuel mainly due to the increase in char content as percentage of tire decreases as tabulated in Table 1. The peak centerline gas temperature is 664K, 620K, 617K, and 611K for 0% tire, 5% tire, 10% tire and 20% tire coal blends respectively as shown in figure 4. The peak centerline gas temperature for the coal gasification decreases by 6.6% when 5% of tire is blended with coal. On the other hand, the effect of tire addition on the amount of CO produced was not found to follow a simple pattern. As depicted in figure 5, it is evident that more CO is produced right next to the inlets (0-3 m axial distance), however, as the reactions progress along the gasifier, different trends are noticed. One reason can be the close ratio of volatiles/char for tires used in this study and the simulation of more than one reaction which makes the prediction of CO produced a function of more than one variable.

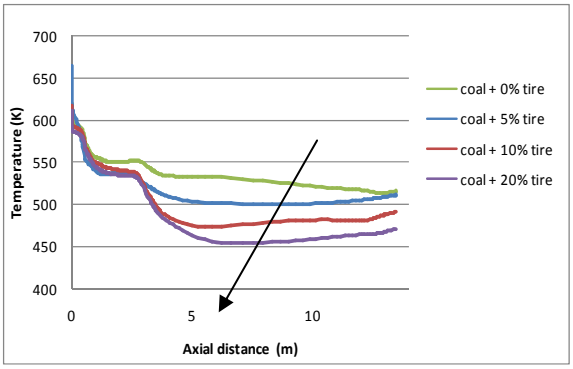

Fig. 4. Centerline gas temperature.

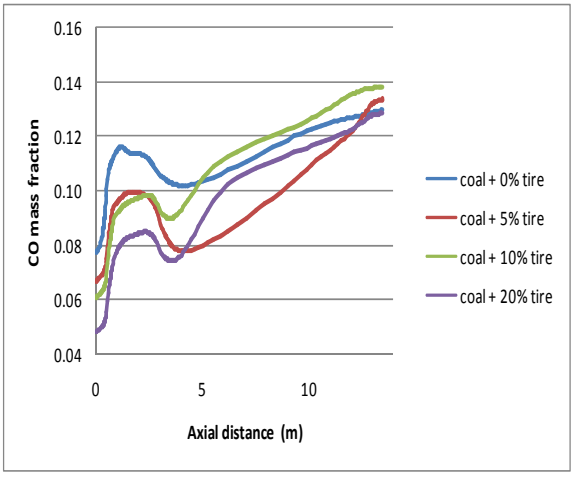

Fig. 5. Centerline CO mass fraction.

Better burnout rates are obtained as shown in figure 6 when tire chips are blended with coal. Compared with the baseline case of 0% tire, tire-coal blends show more homogeneous burnout along the gasifier centerline. Practically, char particles resulting from the devolatilization of tire are more porous than those resulting from coal and hence more reactive.

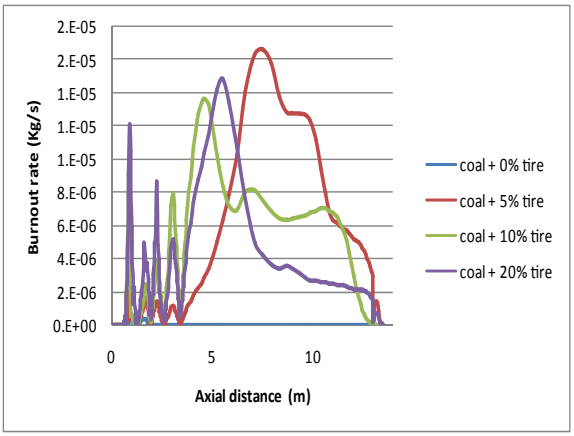

Fig. 6 . Centerline particle burnout rates.

Finally, the effect of adding tire to coal gasification on the pollutant NO production was investigated. Figure 7 shows NO mass fraction for each of the four cases along the gasifier centerline. In this study, it was noted that the NOx emissions consist mostly of NO. In general, the formation of thermal NOx is determined by a set of highly-temperature dependant chemical reactions known as the extended Zeldovich mechanism. For the fuel NOx, the nitrogen containing organic compounds present in the solid fossil fuel can contribute to the total NOx formed during the gasification process. This fuel nitrogen is particularly an important source of nitrogen oxide emissions for coal used in this study, which contains 1.53% nitrogen by weight.

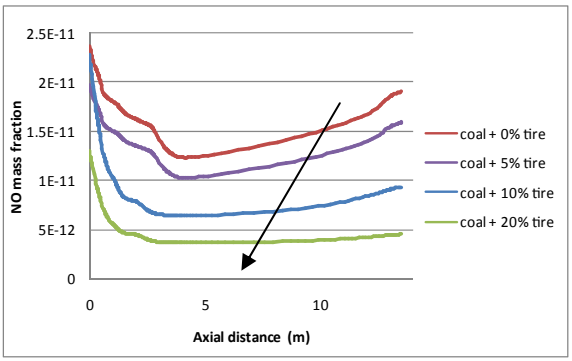

Fig. 7. Mass fraction contours of NO for 0%, 5%, 10% and 20% tire-coal blends.

Similar to the gas temperature, the mass fraction of the NO decreases with the increase in the fraction of tire fuel blended with coal. The NO mass fraction at the gasifier outlet is 1.93×10^{-11}, 1.61×10^{-11}, 9.32×10^{-12}, and 4.53×10^{-12} for 0%, 5%, 10%, and 20% tire-coal fuel blends respectively. NO mass fraction at the outlet decreases by 17% when 5% of tire is blended with coal and by 52% for 10% tire-coal blend. The reduction of NO mass fraction for coal/biomass co-gasification is due to the reduction of both thermal and fuel NOx. In fact the gas temperature decreased by 6.6% for the coal +5% tire compared to coal gasification without tire as depicted previously in figure 4. Consequently, the thermal NOx will also be reduced because it is highly temperature dependent. In addition to that there is also a reduction of fuel NOx for the coal-tire blends because of the net decrease of the amount of nitrogen as summarized in Table 1. The results obtained in this study show clearly the benefits of co-gasification on the reduction of traditional pollutant (NOx).

4. Conclusion

A numerical investigation of co-gasification of coal with 5, 10, and 20% (mass basis) tire is presented in this study. Systematic analysis in addition to CFD using Species Transport model along with discrete phase modeling are used for the investigation of this complex problem that involves gas and particle phases along with the effect of the turbulence on the chemical reactions. Systematic results show negligible effect of blending tire with coal on the production of CO, whereas H_2 and H_2S production increased with higher content of tire. On the other hand, less NH_3 is produced as tire content increases. These results follow the variation of ultimate composition of the fuel as the tire content increases, i.e., as the sulfur content increases with higher percentage of tire, H_2S produced increase. On the other hand, the CFD results were in general agreement with systematic analysis except that they represent a more realistic model which causes some differences compared to the ideal systematic approach. The results show a reduction of gas temperature and the pollutant NO mass fraction as more tire is blended with coal. The producer gas temperature decreased by 6.6% when 5% tire was blended with coal and by 52% when 10% tire was blended. Whereas the effect of blending tire with coal on CO production didn't result in a specific trend, the model showed a general increase in the rate of particle burnout as more homogeneous and stable burnout was noticed for high tire content fuels mainly due to the higher porosity and thus reactivity of char produced from tire than that produced from coal.

References

[1]Boylan, D., Bush, V., and Bransby, D. I., Biomass and Bioenergy, 19 (2000), pp. 411-417.

[2] Freeman, MC., Chister, D.C., James, R.A., Ekmann, J.M., and Walbert, G. F., "Results of pilot-scale Biomass Co-Firing for P.C. Combustors," DOE/FETC, Advanced Coal Base Power & Environmental Systems Conference, 1997, Pittsburgh, Pennsylvania.

[3] Sami, M., Annamalai, K., and Wooldridge, M., Progress in Energy and Combustion Science, 27 (2001), pp. 171-214.

[4] Hein, K.R.G., Bentgen, J.M., "EU clean coal technology, combustion of coal and biomass," Fuel Process Technology, 54 (1998), pp. 159

[5] M. J. Bockelie, M. K. Denison, Z. Chen, T. Linjewile, C. L. Sensior, A. F. Sarofim, "CFD Modeling of Entrained Flow Gasifiers in Version 21 Systems", Report reaction Engineering International, 77 West 200 south, suite 210, Salt Lake City, UT 84101

[6] C. Chen, M. Horio, T. Kojima, Chem. Eng. Science Vol. 55 No. 18, 2000, 3875-3883

[7] C. Chen, M. Horio, T. Kojima, Fuel Vol. 80 , no. 10 , 2001, 1513-1523

[8] M. J. Bockelie, M. K. Denison, Z. Chen, T. Linjewile, C. L. Sensior, A. F. Sarofim, "CFD Modeling of Entrained Flow Gasifiers in Version 21 Systems", Report reaction Engineering

International, 77 West 200 south, suite 210, Salt Lake City, UT 84101

[9] H. Watanabe, M. Otaka, Fuel 85 , 2006), pp. 1935-1943

[10] I. Janajreh, I. Talab, R. Qudaih, "Waste Representation and Numerical Simulation of Entrained Flow Gasifier", Proceedings of the Inaugural US-EU-China Thermophysics Conference, ASME May 28th-30th , Beijing , ChinaUECTC-RE '09.

[11] C. Ghenai, I. Janajreh, "CFD Analysis of the Effects of Co-firing Biomass with Coal", Golabal Conference on Renewable Energy Approaches for Desert Regions March 31st –April 2nd, 2009 Amman Jordan.

[12] C. Ghenai, and I. Janajreh, "Numerical Modeling of Coal/Biomass Co-Firing", FEDSM2008-55204, Symposium on Transport Phenomena in Energy Conversion From Clean and Sustainable Resources Jacksonville, Florida, August 10-14, 2008.

[13] Fluent 6.3.26, Fluent Inc. 2007.